Journal of Radiation Research, Vol. 57, No. 6, 2016, pp. 596–606
doi: 10.1093/jrr/rrw058
Advance Access Publication: 5 July 2016

Dependence and independence of survival parameters on linear energy transfer in cells and tissues

Koichi Ando[1*] and Dudley T. Goodhead[2]

[1]Heavy Ion Medical Center, Gunma University, Showa-machi 3-39-22, Maebashi-shi, Gunma 371-8511, Japan
[2]Medical Research Council, Harwell, Didcot OX11 0RD, UK
*Corresponding author. Heavy Ion Medical Center, Gunma University, Showa-machi 3-39-22, Maebashi-shi, Gunma 371-8511, Japan.
Tel: +81-27-220-8378; Fax: +81-27-220-8379; Email: kando3@gunma-u.ac.jp
Received September 11, 2015; Revised December 23, 2015; Accepted April 20, 2016

ABSTRACT

Carbon-ion radiotherapy has been used to treat more than 9000 cancer patients in the world since 1994. Spreading of the Bragg peak is necessary for carbon-ion radiotherapy, and is designed based on the linear–quadratic model that is commonly used for photon therapy. Our recent analysis using *in vitro* cell kills and *in vivo* mouse tissue reaction indicates that radiation quality affects mainly the alpha terms, but much less the beta terms, which raises the question of whether this is true in other biological systems. Survival parameters alpha and beta for 45 *in vitro* mammalian cell lines were obtained by colony formation after irradiation with carbon ions, fast neutrons and X-rays. Relationships between survival parameters and linear energy transfer (LET) below 100 keV/μm were obtained for 4 mammalian cell lines. Mouse skin reaction and tumor growth delay were measured after fractionated irradiation. The Fe-plot provided survival parameters of the tissue reactions. A clear separation between X-rays and high-LET radiation was observed for alpha values, but not for beta values. Alpha values/terms increased with increasing LET in any cells and tissues studied, while beta did not show a systematic change. We have found a puzzle or contradiction in common interpretations of the linear-quadratic model that causes us to question whether the model is appropriate for interpreting biological effectiveness of high-LET radiation up to 500 keV/μm, probably because of inconsistency in the concept of damage interaction. A repair saturation model proposed here was good enough to fit cell kill efficiency by radiation of wide-ranged LET. A model incorporating damage complexity and repair saturation would be suitable for heavy-ion radiotherapy.

KEYWORDS: carbon ions, LQ, repair saturation, model, cells, tissue

INTRODUCTION

Carbon-ion radiotherapy started in 1994 at the National Institute of Radiological Sciences in Chiba, Japan, and since then more than 9000 patients have been treated with this therapy in the world [1]. Bragg peaks are spread out and provide various LET values along the beam path. Physical dose within the Spread-Out Bragg peak (SOBP) is designed to produce 10% cell kill of the human tumor cell line HSG at any position within a SOBP so that the biological effectiveness will be uniform [2]. It should be noted that a local effect model [3] is being used to design the SOBP in Germany and Italy. A new ridge filter was recently designed based on mouse skin reaction, and it was found that the physical dose distribution required to uniformly cause a given skin reaction score was the same as that required to produce 10% cell kill of HSG cells [4, 5]. The dose range used for the 10% cell kill is ~6 Gy, whereas that for skin reaction is almost 10 times larger, i.e. ~50 Gy, after photon irradiation. Hence, the question arises as to why the same ridge filter could produce uniform effects for different cell/tissue responses, despite the fact that relative biological effectiveness (RBE) of high-LET radiation is not constant and depends on biological endpoints, dose size and survival levels as well. When the survival parameters (alpha and beta) in the linear–quadratic (LQ) model used to design the ridge filter were compared between HSG cells and mouse skin reaction, the alpha terms of the cell and the tissue increased linearly with LET, while this increase was not commonly detected for the

beta terms. This implies that radiation quality affects mainly alpha terms, but much less the beta terms. These two parameters expressed as alpha/beta ratios have been extensively studied for various tumors and normal tissues in animals and patients [6] to develop new treatment planning in photon therapy. Chapman reports that the variation in alpha values after irradiating 10 human tumor cell lines with photons is large (60-fold), while that in square-root of beta values is quite small (0.27-fold) [7]. Therefore, the significance of beta terms is smaller than that of alpha, but the reason is unknown.

We here collected alpha and beta values of photons and compared them with those of high-LET beams, including carbon ions and fast neutrons, for various mammalian cell lines *in vitro* and tissue responses *in vivo*. Analyzing LET dependency of thus-obtained alpha and beta values revealed contradictions with expectations based on common interpretations of the LQ model and therefore called into question its appropriateness for describing cell kill efficiencies of high-LET carbon ions up to 500 keV/μm. A repair saturation (RS) model would instead be appropriate to use for describing lethal effects induced by a wide range of high-LET irradiation.

MATERIALS AND METHODS

Data collection

Survival parameters, including alpha, beta and the radiation dose required to produce 10% surviving fraction (i.e. D10), were collected from either published papers [5, 8–10] or unpublished data. Colony formation after single doses was used for *in vitro* cell killing. Survival data were fitted to the linear–quadratic formula to obtain parameters of alpha and beta. RBE was calculated by comparing isoeffect-doses to produce 10% survival between 200 kVp X-rays and the test ions. For *in vivo* irradiation, C3H female or male mice aged between 10 and 18 weeks were used for skin reaction or tumor growth delay assays, respectively. They were raised under specific pathogen-free conditions prior to irradiation. Right hind legs were locally irradiated either ~7 days after transplantation of NFSa fibrosarcoma cells or ~5 days after hair removal by applying a depilatory [4, 11]. For foot skin reaction, no pretreatment was applied prior to irradiation [12]. The animals involved in these studies were procured, maintained and used in accordance with the Recommendations for Handling of Laboratory Animals for Biomedical Research, compiled by the Committee on the Safety and Handling Regulations for Laboratory Animal Experiments, NIRS, Japan.

Radiation

Reference radiation

For photon irradiation of cultured cells, 200 kVp X-rays were used. Cells were seeded in 25-cm^2 flasks (Nalge Nunc International, Rochester, NY, USA) and incubated for ~2 days before irradiation. For local irradiation of mice, ^{137}Cs gamma rays were used. Five mice were anesthetized with pentobarbital prior to and during irradiation. Doses to mice were given either once a day or fractionated over up to 6 days.

High-LET radiation

Carbon-12 ions were accelerated by either the HIMAC synchrotron, the medical cyclotron at the National Institute of Radiological Sciences (NIRS), Chiba, or the Riken ring cyclotron at Wako, Japan. Exposures were conducted using horizontal carbon beams with a dose rate of ~3 Gy/min. The LET of 290 MeV/u carbon ions obtained by the HIMAC synchrotron was 14 keV/μm at the entrance of a mono-peak and 6-CM SOBP. The depth position along the irradiation path was adjusted by a polymethyl methacrylate range shifter so that various types of LET could be selected to use. For *in vivo* irradiation, the irradiation fields were defined by use of an iron and a brass collimator. Doses were given in the identical ways to those used in the reference radiation. Fast neutrons were obtained by bombarding a thick beryllium target with 30 MeV deuterons by the NIRS cyclotron. Their LET is ~30 keV/μm [12].

Assay

A colony formation assay was used for *in vitro* cultured cells. For human cells, ~14 days of post-irradiation incubation was carried out in a 5% CO_2 incubator at 37°C for either ~10 or ~14 days for rodent or human cells, respectively [5, 8–10]. For *in vivo* tissues, the following three assays were applied to the corresponding tissues. First: either tumors or skin were irradiated with daily fractionation. Second: tumor growth delay was obtained by measuring diameters of a tumor every other day for at least 4 weeks [11]. Third: skin reaction was scored from the eighth day after irradiation and measured till at least the 35th day [13]. Fe-plots of isoeffect doses after fractionated irradiation were used for *in vivo* tissue reactions [14]. Fourth: the TD50 assay was employed to determine cell survival down to ~10^{-7}. Transplanted tumors growing in syngeneic C3H mice were irradiated with 30 MeV fast neutrons and shortly thereafter removed to make single cell suspensions. Tumor take probabilities were determined after the 2-month observation, and used to calculate surviving fractions after irradiation [15].

Models used for data fit

Cell survivals obtained by colony formation were fitted by either the LQ model or a RS model newly proposed here. These days, models of radiation cell kill can be divided into two categories, depending on their explanation of the curvature of the dose response. One is based on the assumption that lesions produced by radiation interact, or combine, with each other to form other lesions that are lethal to the irradiated cells [16]. This lesion interaction is hypothesized by the theory of the dual radiation action LQ model, the repair–misrepair (RMR) model, the lethal–potentially lethal (LPL) model and the more recent giant loop binary lesion (GLOBLE) model [17]. Another category corresponds to a RS mechanism originally proposed by Calkins [18], who hypothesized that a model incorporating repair enzyme kinetics fits well fits to survival of *Tetrahymena* after X-ray irradiation. A RS model hypothesizes that a cell possesses a pool of chemical compounds that can protect the target molecules [16]. The pool is depleted by increasing the dose, and the cell becomes more radiosensitive. Goodhead applied a simple form of RS model to explain the shouldered survival curves of mammalian cells [19]. His model premises are that repairable radiation lesions are produced by one-track action alone, and that the

curvature (shoulder) of cell survival data represents movement of repair kinetics from an unsaturated to partially saturated state of damage. A concept of two-track interaction or sublethal damage, which is commonly presumed in LQ models, is not included in such a RS model, although hybrid models could be formulated. The RS model proposed by Goodhead [19] is:

$$-\ln S = \in (D) = p\,(aD - c0)/\left\{1 - \frac{c0}{aD}\exp\left[kT\,(c0 - aD)\right]\right\}, \quad (1)$$

where S is the surviving fraction of the cell population, D is the dose, a is the proportionality constant for initial yield of substrate lesions that can be repaired by the saturable-repair molecules, p is the proportion of these lesions that would lead to cell death if not repaired, $c0$ is the pool size of repair molecules, and k is a rate constant. The constant a is implicitly dependent on radiation quality. Goodhead recognized that, in addition, a radiation-quality-dependent dose-linear term may be required for lesions that are not repairable by the saturable system, but this was not incorporated into the formalism he presented, even though he predicted his model could explain LET-dependent increase/decrease for RBE of high-LET radiation. Once we applied his simple one-parameter model formalism to the present survival data obtained after irradiation with carbon ions up to 500 keV/μm, we found that fitness of survival curves were not satisfactory at large doses. To overcome this, we have instead reformulated the model equation to incorporate a current concept of complex DNA damage. We considered that the constant a was valid, but a concept of a fixed pool size $c0$ was not appropriate for high-LET radiation. We hypothesized that repairability depends on two factors; (i) pool size of repair molecules and (ii) magnitude of damage complexity. Therefore, we here propose the following new RS model to the *in vitro* cell killing data for carbon ions. The model used here is:

$$S.F. = \exp\left\{\frac{r - a*d}{1 - r*\exp(r - a*d)/(a*d)}\right\}, \quad (2)$$

where $S.F.$, r, a and d are surviving fraction, repairability (arbitrary units), damage complexity and dose, respectively.

In carrying out our fitting to the model we have used the average LET of each beam as the parameter to specify its quality. We recognize the limitations of LET as a unique specification, because the beams are not precisely mono-energetic and so contain a distribution of LET values, and also because it is well established that particles of different mass but the same LET have different track structures [20] and so can result in differences in RBE. Nevertheless, LET provides the best first approximation for exploration of the models.

Statistical analysis

Slopes of LET-alpha and -beta terms were statistically analyzed by Student's t test. When P values for the one-tailed distribution were <0.05, we treated the intergroup difference as significant.

RESULTS

A total of 45 cell lines were irradiated with single doses of either high-LET beams or reference photons. Table 1 shows survival parameters and D10 values for each cell line (Table 1). We here treated three cell lines of HMV-I, HSG and SQ-5 as individual cases and used their original names, even though they were recently reported as cross-contaminated with HeLa cells [21]. Alpha values for X-rays ranged from 0.032 Gy^{-1} (KNS-60 human medulloblastoma) to 1.776 Gy^{-1} (SX10 mouse squamous cell carcinoma), while beta values varied between 0.009 Gy^{-2} (KNS-89 human gliosarcoma) and 0.156 Gy^{-2} (AT5BIVA human fibroblast). So, the corresponding range of variation was 56- or 17-fold for alpha or beta values, respectively. For high-LET radiation, alpha ranged from 0.299 Gy^{-1} (Sq1979 mouse squamous cell carcinoma) to 2.384 Gy^{-1} (SX10 mouse squamous cell carcinoma), and beta varied from 0.0058 Gy^{-2} (HMV II human malignant melanoma) to 0.405 Gy^{-2} (ONS76 human medulloblastoma). The range of variation for high-LET radiation was 8-fold or 70-fold for alpha or beta values, respectively. The relation between alpha and beta for the fold change of each cell line was negligible (data not shown). The cumulative incidences of alpha and beta values in increasing order of magnitude was then calculated and compared between X-rays and high-LET radiation (Fig. 1). A clear separation between X-rays and high-LET radiation was observed for alpha values, so that the cumulative incidence for high-LET radiation apparently shifted to the right of that for X-rays. On the other hand, the cumulative incidences of beta values were almost the same for X-rays and high-LET radiation, indicating that increase in LET does not change the range of beta values from those of X-rays. The cumulative incidence of alpha/beta ratios for X-rays shifted to the right when cells were irradiated with high-LET radiation, although the shift was less prominent than that observed in alpha values.

We then studied relationships between LET and survival parameters. For this analysis, the following cell lines were used: HSG human salivary gland tumor, T1 human kidney cell, NHDF normal human dermal fibroblasts. Figure 2a shows that alpha values increase with increasing LET up to <100 keV/μm for each of the cell lines. The slope difference between HSG cells and other cells was statistically significant for all alpha and beta, except beta of T1 cells. Similarly, the LET-dependent increase in the alpha term was also observed for *in vivo* tissue early response, including mouse skin reaction and tumor growth delay (Fig. 2b). Slope difference between foot skin after monopeak radiation and other tissues was not significant for any alpha and beta. For beta values, T1 ($P = 0.0001$) and NHDF ($P = 0.0015$) cells clearly show an increase with increasing LET, while independence of LET was shown for HSG cells ($P = 0.096$) and V79 ($P = 0.398$) cells (Fig. 2c). This varying LET dependence of beta was also observed for tissue response such that, for skin reaction, beta increases with an increase in LET ($P = 0.067$, monopeak foot; $P = 0.003$, SOBP foot; $P = 0.082$, SOBP leg) while for tumor growth delay, beta was independent of LET ($P = 0.25$) (Fig. 2d).

The above-stated results raise a fundamental question as to why LET strongly affects alpha terms but not beta. It is now generally accepted that high-LET radiation induces complex clustered damage

Table 1. Cell lines used to obtain Fig. 1

Cell line	Histology	Origin	X-rays			Ions		
			alpha (Gy^{-1})	beta (Gy^{-2})	D10 (Gy)	alpha (Gy^{-1})	beta (Gy^{-2})	D10 (Gy)
Carbon-ions 55 keV/μm								
92-1	malignant melanoma	human	0.880 75	0.067 67	2.235 24	1.306 07	0.085 45	1.597 35
HMV-I	malignant melanoma	human	0.117 74	0.076 90	4.807 10	0.460 79	0.138 90	2.736 68
MeWo	malignant melanoma	human	0.529 65	0.044 34	3.397 10	0.962 52	0.034 88	2.215 97
HMV-II	malignant melanoma	human	0.290 44	0.018 68	5.800 29	0.682 68	0.005 81	3.282 37
C32TG	malignant melanoma	human	0.198 37	0.045 40	5.255 21	0.713 67	0.058 10	2.655 94
Colo679	malignant melanoma	human	0.170 25	0.071 42	4.636 22	0.618 59	0.057 46	2.927 61
G361	malignant melanoma	human	0.079 38	0.067 44	5.300 60	0.428 28	0.103 70	3.081 09
OMM-1	malignant melanoma	human	0.101 21	0.043 17	6.223 69	0.491 37	0.052 05	3.442 34
GAK	malignant melanoma	human	0.185 28	0.015 46	7.582 37	0.367 88	0.018 79	4.984 42
SQ-5	squamous cell carcinoma	human	0.330 77	0.033 97	4.696 70	0.771 66	0.049 16	2.564 06
HSQ-89	squamous cell carcinoma	human	0.222 20	0.037 14	5.475 65	0.543 68	0.057 37	3.178 30
Carbon-ions 77 keV/μm								
LC-1 sq	squamous cell carcinoma	human	0.244 60	0.127 10	3.41	1.461 00	0.061 04	1.48
A-549	adenocarcinoma	human	0.074 56	0.045 48	6.34	0.720 60	0.051 60	2.68
C32TG	melanoma	human	0.250 80	0.039 59	5.09	1.123 00	0.016 09	1.99
Marcus	astrocytoma	human	0.177 70	0.047 37	5.35	0.732 60	0.137 20	2.22
SM-MG-1	astrocytoma	human	0.109 50	0.052 92	5.64	0.619 40	0.128 60	2.46
KNS-89	gliosarcoma	human	0.052 79	0.089 83	4.77	0.644 50	0.149 50	2.32
ONS-76	medulloblastoma	human	0.095 84	0.090 21	4.55	0.664 00	0.405 10	1.70
KNS-60	glioma	human	0.031 56	0.048 16	6.59	0.815 60	0.040 56	2.51
Becker	astrocytoma	human	0.100 00	0.022 41	8.15	0.316 30	0.072 61	3.86
T98G	glioblastoma	human	0.063 73	0.046 15	6.41	0.432 40	0.089 50	3.20
SF126	astrocytoma	human	0.211 30	0.063 84	4.58	0.894 80	0.088 40	2.13
HSG	salivary gland tumor	human	0.331 20	0.059 26	4.04	1.402 70	0.029 07	1.59
Fast neutrons								
R1	embryonic stem cell	mouse	0.052 16	0.067 07	5.483 3	0.482 7	0.089 48	3.048
HSG	salivary gland tumor	human	0.331 2	0.059 26	4.036 7	0.954 9	0.087 6	2.0324
V79		Chinese hamster	0.167 4	0.025 6	6.762 1	0.583	0.018 59	3.548 1
HeLaS3		human	0.527	0.010 4	4.046 2	0.667	0.086 5	2.585 3

Continued

Table 1. Continued

Cell line	Histology	Origin	X-rays			Ions		
			alpha (Gy^{-1})	beta (Gy^{-2})	D10 (Gy)	alpha (Gy^{-1})	beta (Gy^{-2})	D10 (Gy)
Sq1979		mouse	0.034 9	0.038 9	7.258 1	0.299	0.038 4	4.774
irs3		Chinese hamster	0.448 36	0.015 36	4.455	0.75631	0.027	2.770 5
LY-S		mouse	1.018	0.102	1.900 1	1.508	0.134	1.362 1
MRC5sv1TG1		human	0.265 68	0.033 37	5.230 5	0.59345	0.048 85	3.092 7
irs2		Chinese hamster	0.652 65	0.052 82	2.864	1.0173	0.076 96	1.969 8
AT5BIVA	fibroblast	human	1.020 4	0.155 93	1.775 1	2.1767	0.021 6	1.046 9
A7		human	0.295 2	0.025 03	5.362 1	0.762	0.092 9	2.349
L5178Y		mouse	0.295 2	0.075	3.912	0.6102	0.175 5	2.279 3
SX10	squamous cell carcinoma	mouse	1.776 4	0.081 71	1.227	2.3836	0.095 08	0.931 41
SX9		mouse	1.011 3	0.065	2.015 7	1.4127	0.116 39	1.455 4

Survival parameters (alpha and beta) and a dose required to reduce surviving fraction to 10% (D_{10}) are included for reference X-rays and high-LET radiations (carbon ions with 55 or 77 keV/μm, 30 MeV fast neutrons).

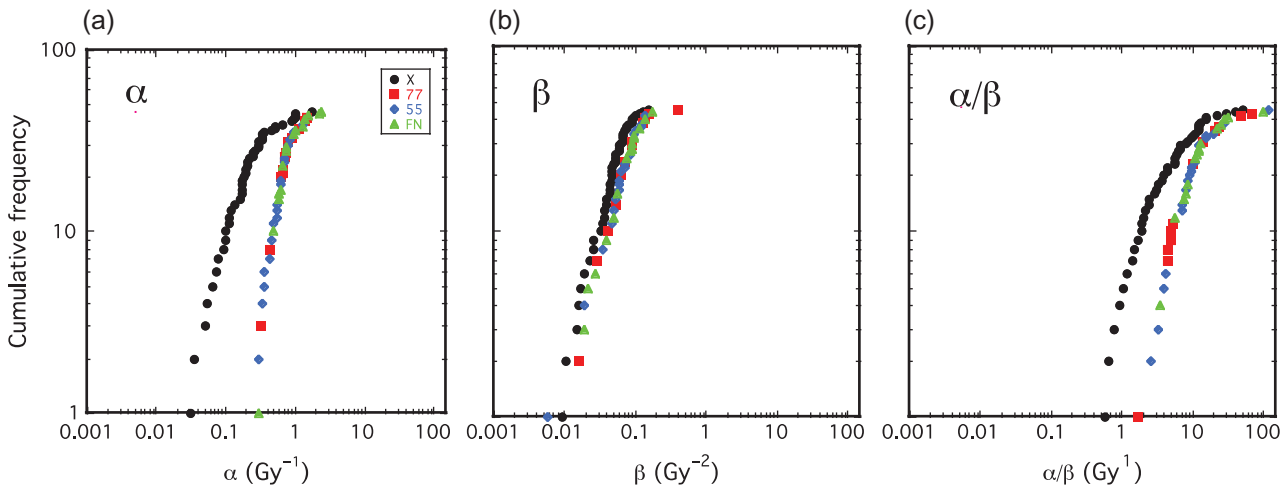

Fig. 1. Cumulative incidence of survival parameters. The survival parameters of 45 cell lines listed in Table 1 are used to compare between low- and high-LET radiations. Horizontal scales are alpha (a), beta (b) and alpha/beta ratio (c). The vertical scale is the cumulative incidence of each parameter. Colors red and black are for photons and ions, respectively. Left panel is for alpha, middle for beta and right for α/β ratio, respectively.

to DNA, particularly complex double-stranded breaks (DSBs) [22–25], which are less repairable by either non-homologous end-joining or the homologous recombination pathway [26]. Throughout this paper, 'clustered damage' to DNA is intended to refer only to damage at the nanometer level of the DNA molecule, mostly extending over not more than one or two helical turns of the DNA, in accordance with the original usage of the term in the references cited. It is not intended to include correlated or associated damage that may occur, from either single- or multi-track action, to more distant parts of the same DNA molecule, hundreds, thousands or millions of base-pairs away, which have also sometimes been referred to in published literature as 'clustered damage'. It is very strange that clustered damage to DNA affects only alpha terms, dominant at low doses, but does not much affect beta terms at high doses, while the proportion of complex clustered DNA damage, relative to more simple damage, should be induced in cells irrespective of dose size since it is produced by individual radiation tracks. If, in accordance with current knowledge, the total yield of DSBs increases with LET, the

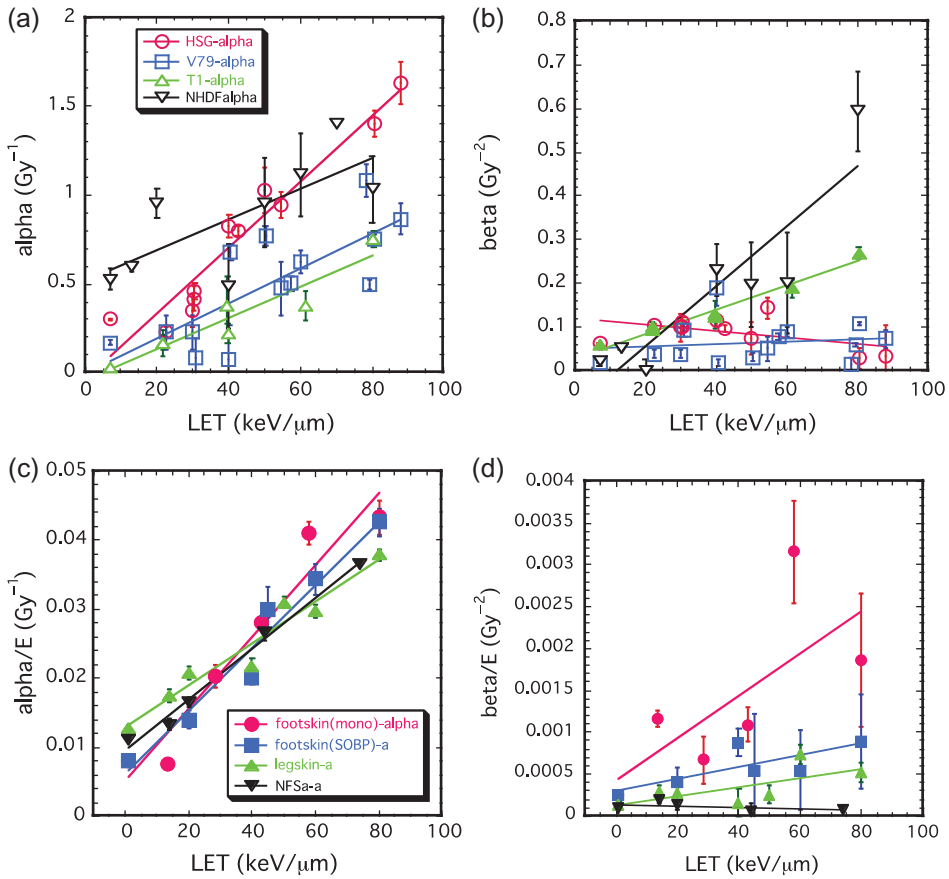

Fig. 2. Dependence of survival parameters on LET. The survival parameters of alpha and beta are plotted against various LET of carbon ions up to 100 keV/μm. Cell lines named HSG, T1 and NHDF are from human, while V79 is from Chinese hamster. For the *in vivo* response, C3H mice were used. Skin (leg or foot) and a transplanted tumor were used, and mono and SOBP refer to monopeak beams and Spread-Out Bragg peak beams, respectively. The LET distribution in monopeak beams is narrower than that in SOBP. (a) alpha for cultured cells, (b) alpha terms for *in vivo* tissues, (c) beta for cultured cells, (d) beta terms for *in vivo* tissues. 'E' in vertical scale is surviving fraction corresponding to observed response, but not identifiable by the Fe-Plot. Symbols and bars are means and standard deviations. For the slopes, mean and standard deviation for alpha are: 0.011 ± 0.011 (HSG), 0.0052 ± 0.0058 (V79), 0.0013 ± 0.0013 (T1), 0.883 ± 0.0320 (NHDF), 0.0016 ± 0.0032 (monopeak foot skin), 0.0015 ± 0.0032 (SOBP foot skin), 0.0022 ± 0.0047 (SOBP leg skin) and 0.0026 ± 0.0048 (NFSa tumor). *P* values for beta are; 0.0023 ± 0.0023 (HSG), 0.00057 ± 0.00063 (V79), 0.0026 ± 0.0027 (T1), 0.173 ± 0.191 (NHDF), 0.00005 ± 0.00001 (monopeak foot skin), 0.00005 ± 0.00001 (SOBP foot skin), 0.00002 ± 0.00005 (SOBP leg skin) and 0.00002 ± 0.00004 (NFSa tumor). *P* values between HSG cells and other cells are: 0.054 and 0.007 (V79), 0.019 and 0.39 (T1) and 0.028E-6 and 0.004 (NHDF) for alpha and beta, respectively. *P* values between monopeak foot skin and other tissues are: 0.49 and 0.49 (SOBP foot skin), 0.394 and 0.3284 (SOBP leg skin) and 0.256 and 0.28 (NFSa tumor) for alpha and beta, respectively.

proportion of DSB that are complex increases with LET, the degree of complexity of the complex DSB increases with LET, and/or if complex DSB are more persistent and more likely to be misrepaired, one might expect the beta term to be increased (according to the square of the initial yield of the relevant sublesions in the simplest sublesion–interaction models) as the LET increases, as well as the alpha term being increased. This raises a fundamental puzzle or contradiction in common interpretations of the LQ model.

For further investigation, the new RS model was fitted to the *in vitro* cell killing data for carbon ions. As shown in Fig. 3, survival curves fitted by the RS model are indistinguishable from those fitted by the LQ model. After fitting to all survival data obtained after various LET of carbon ions up to 500 keV/μm, survival parameters of the RS model (i.e. r and a) were compared with those of the LQ model (alpha and beta). LET dependence of either damage complexity or alpha is observed for HSG cells and V79 cells (Fig. 4a and b). Both a and alpha values increase with an increase in LET up to ~150 keV/μm, reach a peak, and then decrease with further increase of LET. The peak position for HSG cells locates at marginally lower LET for the RS model than the LQ model, while the peak for V79 cells seems higher for the RS model than for LQ. The alpha-parameter of the LQ-model is much more sensitive than the

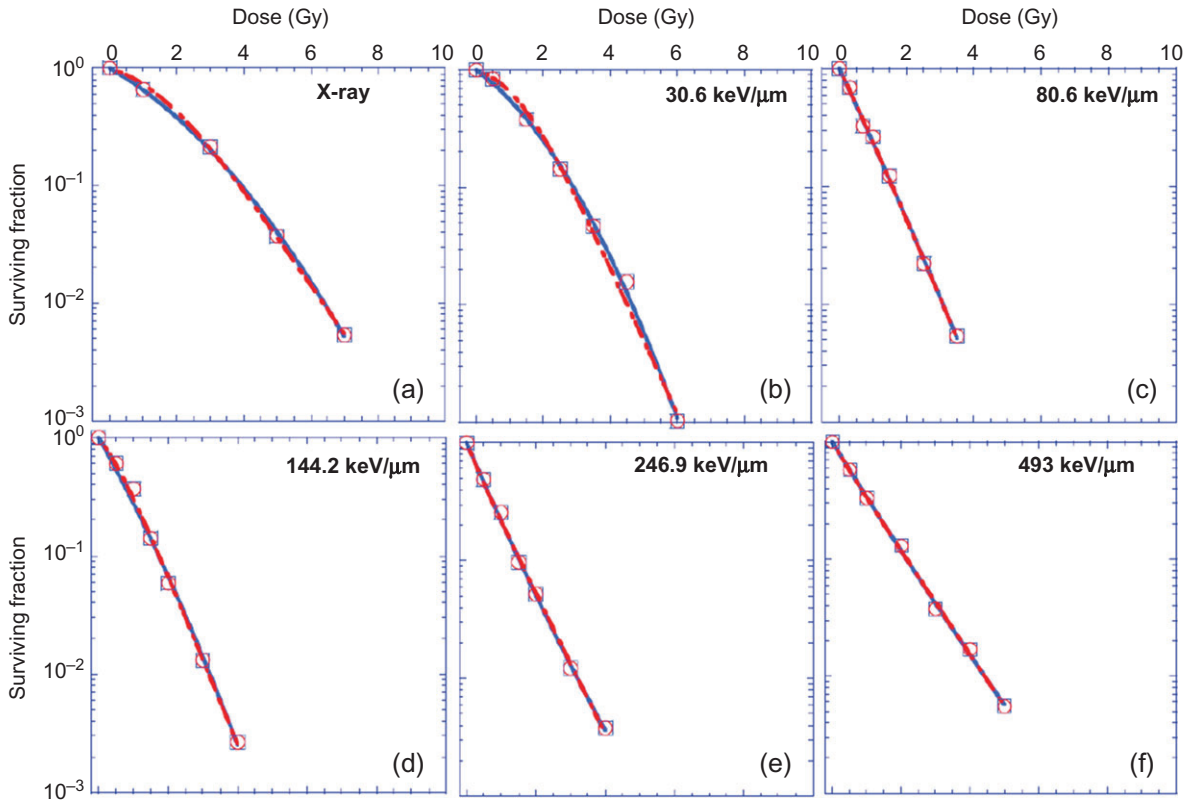

Fig. 3. Examples of curve fit by the LQ model and the RS model applied to HSG cells. The color blue is for the RS model, while red is for the LQ model. Panels are (a) X-rays or carbon ions with (b) 30.6 keV/μm, (c) 80.6 keV/μm, (d) 144.2 keV/μm, (e) 246.9 keV/μm or (f) 493.0 keV/μm, respectively.

a-parameter of the RS model. The former varies by a factor of ~15–20 within the LET range from 0–150 keV/μm; the corresponding change in the parameter *a* of the RS model is only of the order of 1.5–2. On the other hand, the repairability parameter (*r*) of the RS model shows LET dependence substantially different from that of the beta parameter of the LQ model (Fig. 4c, d, e and f). The *r* values of either HSG or V79 cells decrease with an increase in LET up to ~150 keV/μm, over which *r* values stay at ~0, while the beta values do not depend on LET up to 500 keV/μm staying around zero. It is noticed that V79 cells show larger *r*-values than HSG cells for low-LET radiation. When plotted against survival parameters, the RBE values of HSG cells increase linearly with an increase in either *a* or alpha values; the latter shows a shallower slope than the former (Fig. 5a). The RBE values of HSG cells decrease with an increase in either *r* or beta values; a steeper slope is observed for the latter than the former (Fig. 5b). RBE for V79 cells also increases with an increase in *a* and alpha. However, in contrast to HSG cells, the slope of increase is steeper for alpha than for *a* (Fig. 5c). RBE decreases with an increase in *r*, while beta shows a narrow range of decrease (from −0.0011 to 0.255 Gy^{-2}) such that almost no dependence on beta is apparent graphically (Fig. 5d).

Whether and how well the two models fit to cell survival fractions right down to 10^{-7} was studied for the NFSa tumor. Figure 6 compares the two models. Either the RS or the LQ model fits well to all surviving fractions, even though the correlation coefficients for the LQ model are slightly larger (0.83 for neutrons, 0.84 for gamma rays) than those for the RS model (0.75 for neutrons, 0.76 for gamma rays). Surviving fractions at the 50% tumor control probability (TCD_{50}) were calculated by using the two models; TCD 50 values after fast neutrons and gamma rays were 28.2 Gy and 83.2 Gy, respectively [15]. Surviving fractions at TCD_{50} of gamma rays were calculated as 0.58×10^{-8} and 1.48×10^{-8}, according to the LQ and RS models, respectively, while corresponding fractions for fast neutrons were 1.14×10^{-8} and 3.05×10^{-8}. Therefore, the RS model results in three times higher survival fractions than the LQ model.

DISCUSSION

We analyzed cell-killing data obtained after irradiation with high-LET carbon ions, and compared between two cell survival models for fitting of these data. Results were that either model fits the cell survivals well, but some differences between them were observed. The most prominent difference was in interpretation of the underlying damage process as having dose-squared or dose-linear dependence and the choice of appropriate parameter to use. The RS model used here is based on Michaelis–Menton kinetics [27]. The kinetics is, in short, based on simple reaction between substrate and enzyme such that the velocity of reaction depends on the concentrations of

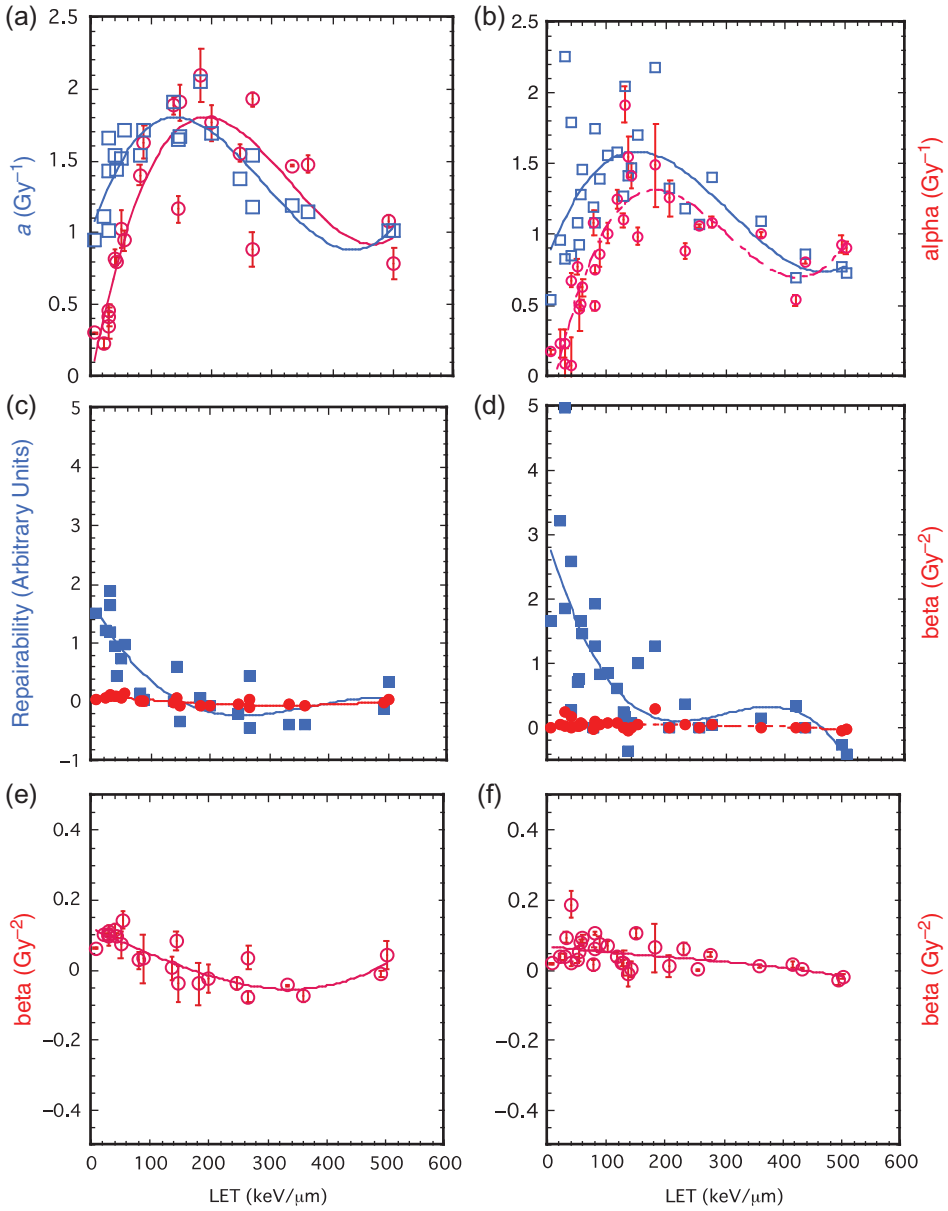

Fig. 4. Comparison between the LQ- and the RS model. Survival parameters obtained by the LQ model (red) and the RS model (blue) are plotted against a wide range of LET up to 500 keV/μm of carbon ions. Panels are HSG cells (a, c, e), V79 cells (b, d, f), alpha and a (a, b), beta and repairability (c, d) or beta covering a range between 0 and 0.5 (e, f), respectively. Symbols and bars are means and standard deviations.

substrate and available enzyme. When substrate concentration is low enough, the enzyme reacts effectively with 100% of the substrate. If the substrate is increased and depletes the enzyme concentration, some or all of the substrate remains unmodified at later times. For radiation-induced cell killing, substrate and enzyme could be replaced by radiation-induced damage and the cell's repair machinery, respectively. Increase in residual damage corresponds to decrease in surviving fraction, while concentration of initial damage corresponds to radiation dose [19]. The present RS model was made by modifying Goodhead's original 1985 model. His model included a single parameter, *a*, for proportionality of initial damage with dose, with *a* being implicitly for radiation quality. The pool size of repair molecules, 'c', in his model was constant for a given cell system and not fitted as a variable. His model fitted well simultaneously to hard and carbon ultrasoft X-ray data [19], but it was not applied to data for a wide range of LET, such as those used in the present study. He suggested that to do so would require an additional dose-linear radiation-quality-dependent term for different damage that was not substrate for the saturable repair system. As curve-fitting using his simple one-parameter model to the present

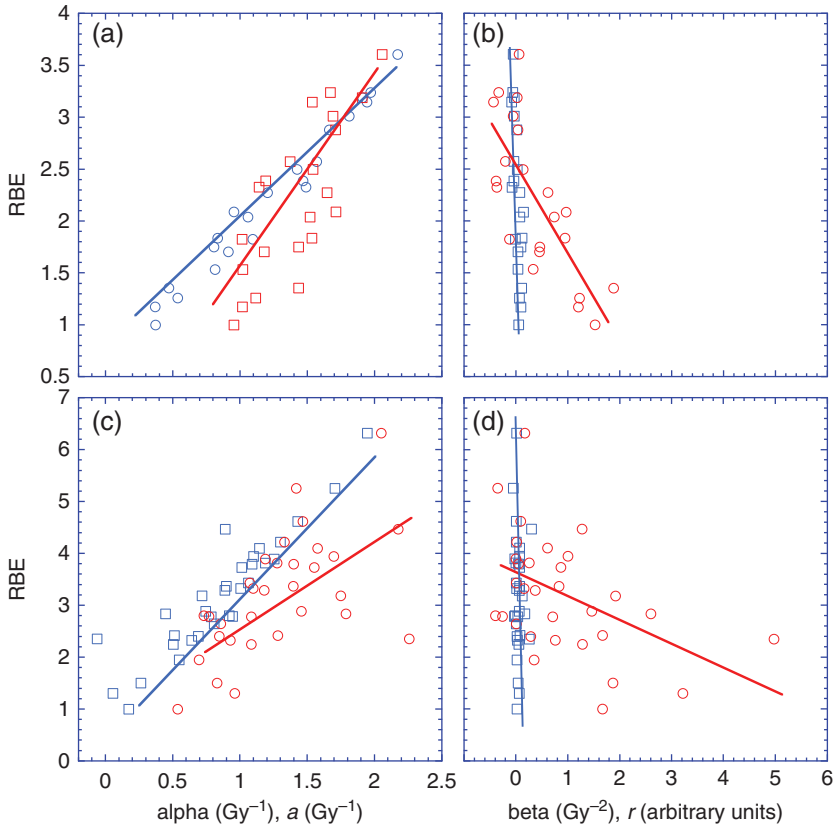

Fig. 5. Survival parameters and RBE for HSG cells. RBE values are plotted against survival parameters. Panels are RBE against alpha and a (a, c), beta and repairability (b, d), for (a, b) HSG cells and (c, d) V79 cells, respectively. In panels a through d, blue is for the LQ model, while red is for the RS model.

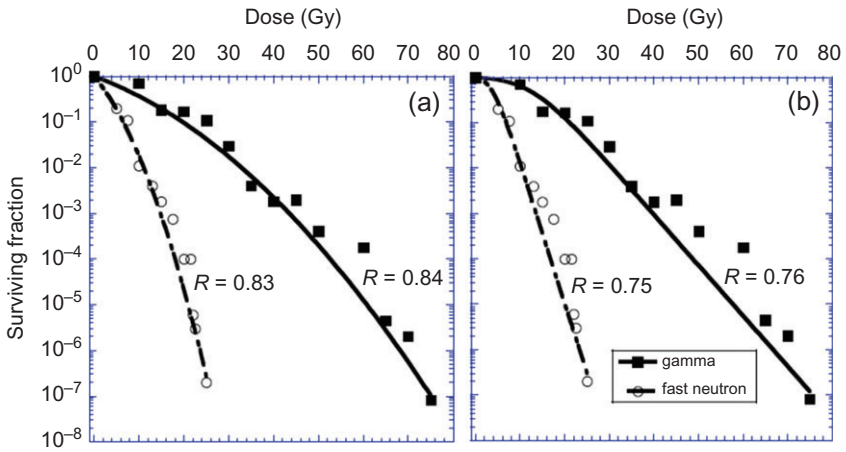

Fig. 6. Cell survivals down to 10^{-7} surviving fraction after gamma rays and fast neutrons. NFSa fibrosarcomas were irradiated with either gamma rays or 30 MeV fast neutrons. Irradiated cells were transplanted to syngeneic mice, and TD50 values determined 2 months later were used to obtain surviving fractions at given radiation doses. Data shown in [13] are fit by (a) LQ model and (b) RS model. Symbols are closed squares: gamma rays, closed circles: fast neutrons, respectively.

high-LET radiation was not satisfactory (data not shown), we modified his model so that the 'c' in his 1985 model was changed to become a variable. That is because efficiency of repair machinery would be limited by damage complexity that depends on radiation quality, even though its pool size is constant. Knowledge of the nature and repair of DNA-DSBs by year 1985 was substantially less than it is today. From earlier biophysical analyses, it had been hypothesized that the increased RBE of high-LET radiations was due primarily to their efficiencies at creating more substantial ionization clusters on the scale of the DNA helix [28], leading to the concept of clustered DNA damage (also sometimes known as locally multiple damage sites (LMDA) [28]. It was proposed that final cellular effects from high-LET radiations are dominated by their more severe, and therefore less repairable, complex clustered damages, and that these can be qualitatively different from the less-complex clustered damage that dominates low-LET effects [29]. Clustered damage is a unique class of DNA lesions that includes two or more individual lesions within one or two helical turns of the DNA (illustrated in reference [25]). These elementary lesions can be strand breaks, abasic sites (apurinic/apyrimidinic sites or APs) or damaged bases (oxidized purines or pyrimidines) [30]. Unrepaired clustered DNA lesions, particularly complex DSBs, induce chromosome breakage in human cells [31].

Within recent decades, molecular mechanisms involved in repair of radiation damage have been clarified such that two pathways to repair radiation-induced DNA-DSBs have been identified in mammalian cells [32]. Non-homologous end-joining works mainly during G1and S phases, while homologous recombination does so in late S and G2 phases. Photon radiation induces predominantly relatively simple DNA-DSBs, while more complex damage is caused by high-LET radiation [23, 33]. Using foci made by replication protein A (RPA) as an indicator of DSB resection, Averbeck *et al.* report that severity of complex damage increases with LET higher than ~150 keV/μm in G1 or S/G2 mammalian cells [34]. This report agrees with the present results that repairability decreased with an increase in LET up to ~150 keV/μm, reaching a minimum of zero (Fig. 4c, d). Also, the decreasing portion in the LET versus *a* (or the LET versus alpha) relation (Fig. 4a and b) would be due to overkill.

The LQ model was proposed by Kellerer and Rossi in 1972 [35]. They hypothesized that RBE of various ionizing radiations is proportional to the square of the local energy concentration within micrometer-scale regions, due to both single and pairs of radiation tracks. This model was further advanced by Hawkins in 1996 [36, 37]. He claimed that cellular processes that repair the primary lesions or convert them to lethal lesions are unaffected by LET, and beta values of high-LET neutrons do not differ from those of photons. In reasonable agreement, the present study showed that beta is essentially independent of LET, while alpha apparently depends strongly on LET. However, the question is: if high-LET radiation induces complex DNA-DSBs that are more difficult to repair, why is the induction of such complex DNA-DSBs apparent only in the low-dose parameter (alpha) and not at high doses (beta)? Therefore, the present study does not support the concept of underlying dose-squared dependence. Extending this question further raises another: whether sublethal damage exists? This is because dose-squared dependence corresponds to interaction of two sublesions caused by two tracks of ionizing radiation [38]. The second question was also raised by Goodhead as early as 1985, and would be answered by using a RS model [19]. In fact, a treatment with cyclophosphamide (a protein synthesis inhibitor) after an initial photon dose reduces the initial shoulder of survival curves and suppresses subsequent second-dose survivals of CHO cells [39]. This supports, at least, the view that DNA-DSB repair proteins are required for sublethal damage to be detected. The LQ assumes binary misrepair to be responsible for the beta term, but it does not explicitly take account of the repair processes or allow for dose dependency of available proteins.

Figure 3 shows similarity of curve fitting between the LQ and RS models. However, there are major differences between the models in interpretation and consequences of their parameters. Consider, for example, two survival curves that have substantial real differences, even though for similar LET (as can be seen in Fig. 3), the differences being predominantly in the initial slopes: for the LQ model fits, this difference is expressed almost entirely by the alpha parameters (i.e. initial slope parameter), while for the RS model it is shared between the damage complexity (*a*) and repairability (*r*) parameters since the initial slope is a function of both, as has been pointed out by Goodhead [19]. For the RS model, the RBE is determined more equally by *both* the parameters and so neither one *alone* correlates strongly with the RBE. Accordingly, Fig. 5 shows the variability of alpha is smaller than that of *a*. This is mostly due to the strong role played by the initial slope in all the high-LET survival curves; in the LQ model the initial slope is defined by alpha alone, whereas in the RS model the initial slope depends on both parameters (*a* and *r*).

As any SOBP of charged-particle radiotherapy inevitably consists of mixed LET, the way damage complexity is handled by the RS model will vary. Further understanding of this model will require collaboration of mathematics and biology for its future advancement.

ACKNOWLEDGEMENTS

We are grateful to Dr Yoshiya Furusawa, Dr Yoshitaka Matsumoto, Dr Masao Suzuki, Dr Kiyomi Eguchi-Kasai and Dr Yukari Yoshida for providing cell survival data. Data from this study was presented at the 15th International Congress of Radiation Research, held 25–29 May, 2015 in Kyoto, Japan.

FUNDING

This report is partly supported by the Special Coordination Funds for Research Project with Heavy Ions at the National Institute of Radiological Sciences–Heavy-ion Medical Accelerator in Chiba (NIRS-HIMAC).

CONFLICT OF INTEREST

The authors declare that there are no conflicts of interest.

REFERENCES

1. Jermann, M. Particle therapy statistics in 2013. *Int J Particle Ther* 2014;1:40–3.
2. Kanai T, Endo M, Minohara S, et al. Biophysical characteristics of HIMAC clinical irradiation system for heavy-ion radiation therapy. *Int J Radiat Oncol Biol Phys* 1999;44:201–10.

3. Scholz M, Kraft G. Calculation of heavy ion inactivation probabilities based on track structure, X ray sensitivity and target size. *Radiat Prot Dosimetry* 1994;52:29–33.
4. Uzawa A, Ando K, Kase Y, et al. Designing a ridge filter based on a mouse foot skin reaction to spread out Bragg-peaks for carbon-ion radiotherapy. *Radiother Oncol* 2015;115:279–83.
5. Furusawa Y, Fukutsu K, Aoki M, et al. Inactivation of aerobic and hypoxic cells from three different cell lines by accelerated ^{3}He-, ^{12}C- and ^{20}Ne-ion beams. *Radiat Res* 2000;154:485–96.
6. Bentzen SM, Joiner MC. The linear–quadratic approach in clinical practice. In: Joiner M, van der Kogel A (eds). *A Basic Clinical Radiobiology*. 4th edn. London: Hodder Arnold, 2009, 120–34.
7. Chapman JD. Can the two mechanisms of tumor cell killing by radiation be exploited for therapeutic gain? *J Radiat Res* 2014;55:2–9.
8. Matsumoto Y, Iwakawa M, Furusawa Y, et al. Gene expression analysis in human malignant melanoma cell lines exposed to carbon beams. *Int J Radiat Biol* 2008;84:299–314.
9. Suzuki M, Kase Y, Yamaguchi H, et al. Relative biological effectiveness for cell-killing effect on various human cell lines irradiated with heavy-ion medical accelerator in Chiba (HIMAC) carbon-ion beams. *Int J Radiat Oncol Biol Phys* 2000;48:241–50.
10. Eguchi-Kasai K, Murakami M, Itsukaichi H, et al. The role of DNA repair on cell killing by charged particles. *Adv Space Res* 1996;18:109–18.
11. Ando K, Koike S, Urawa A, et al. Biological gain of carbon-ion radiotherapy for the early response of tumor growth delay and against early response of skin reaction in mice. *J Radiat Res* 2005;46:51–7.
12. Ito A, Henkelman RM. Microdosimetry of the pion beam at TRIUMF. *Radiat Res* 1980;82;413–29.
13. Ando K, Koike S, Nojima K, et al. Mouse skin reactions following fractionated irradiation with carbon ions. *Int J Radiat Biol* 1998;74:129–38.
14. Douglas BG, Fowler JF. The effect of multiple small doses of X rays on skin reactions in the mouse and a basic interpretation. 1976. *Radiat Res* 2012;178:AV125–38.
15. Ando K, Koike S, Sato S. Nonlinear survival curves for cells of solid tumors after large doses of fast neutrons and gamma rays. *Radiat Res* 1992;131:157–61.
16. Sanchez-Reyes A. A simple model of radiation action in cells based on a repair saturation mechanism. *Radiat Res* 1992;130:139–47.
17. Herr L, Friedrich T, Durante M, et al. A comparison of kinetic photon cell survival models. *Radiat Res* 2015;184:494–508.
18. Clkins J. A method of analysis of radiation response based on enzyme kinetics. *Radiat Res* 1971;45:50–62.
19. Goodhead DT. Saturable repair models of radiation action in mammalian cells. *Radiat Res Suppl* 1985;8:S58–67.
20. Kraft G, Kramer M, Scholz M. LET, truck structure and models. *Radiat Environ Biophys* 1992;31:161–80.
21. Capes-Daviz A, Theodosopoulos G, Atkin I, et al. Check your cultures! A list of cross-contaminated or misidentified cell lines. *Int J Cancer* 2010;127:1–8.
22. Hada M, Georgakilas AG. Formation of clustered DNA damage after high-LET irradiation: a review. *J Radiat Res* 2008;49:203–10.
23. Davis AJ, Chen DJ. Complex DSBs: a need for resection. *Cell Cycle* 2014;13:3796–7.
24. Goodhead DT. Initial events in the cellular effects of ionizing radiations: clustered damage in DNA. *Int J Radiat Biol* 1994;65:7–17.
25. Goodhead DT. Fifth Warren K. Sinclair keynote address: issues in quantifying the effects of low-level radiation. *Health Phys* 2009;97:394–406.
26. Hufnagl A, Herr L, Friedrich T, et al. The link between cell-cycle dependent radiosensitivity and repair pathways: a model based on the local, sister-chromatid conformation dependent switch between NHEJ and HR. *DNA Repair* 2015;27:28–39.
27. Dowd JE, Riggs DS. A comparison of estimates of Michaelis–Menton kinetic constants from various linear transformations. *J Biol Chem* 1965;240:863–9.
28. Ward JF. Biochemistry of DNA lesions. *Radiat Res* 1985;104:S103–11.
29. Goodhead DT, Thacker J, Cox R. Weiss lecture: effects of radiations of different qualities on cells: molecular mechanisms of damage and repair. *Int J Radiat Biol* 1993;63:543–56.
30. Lomax ME, Folkes LK, O'Neill P. Biological consequences of radiation-induced DNA damage: relevance to radiotherapy. *Clin Oncol* 2003;25:578–85.
31. Asaithamby A, Hu B, Chen DJ. Unrepaired clustered DNA lesions induce chromosome breakage in human cells. *Proc Natl Acad Sci USA* 2011;108:8293–8.
32. Shrivastav M, De Haro LP, Nickoloff JA. Regulation of DNA double-strand break repair pathway choice. *Cell Res* 2008;18:134–47.
33. Goodhead DT. Energy deposition stochastics and track structure: what about the target? *Radiat Prot Dosim* 2006;122:3–15.
34. Averbeck NB, Ringel O, Herrlitz M, et al. DNA end resection is needed for the repair of complex lesions in G1-phase human cells. *Cell Cycle* 2014;13;2509–16.
35. Kellerer AM, Rossi HH. The theory of dual radiation action. In: Ebert M, Howard A (eds). *Current Topics in Radiation Research Quarterly*, Vol. 8, Amsterdam: North-Holland Publishers, 1972, 85–158.
36. Hawkins RB. A statistical theory of cell killing by radiation of varying linear energy transfer. *Radiat Res* 1994;140:366–74.
37. Hawkins RB. A microdosimetric–kinetic model of cell death from exposure to ionizing radiation of any LET, with experimental and clinical applications. *Int J Radiat Biol* 1996;69:739–55.
38. Park C, Papiez L, Zhang S, et al. Universal survival curve and single fraction equivalent dose: useful tools in understanding potency of ablative radiotherapy. *Int J Radiat Oncol Biol Phys* 2008;70:847–52.
39. Yezzi MJ, Blakely EA, Tobias CA. Split-dose recovery and protein synthesis in X-irradiated CHO cells. *Radiat Res* 1988;114:281–96.